

# FOSS: Multi-Person Age Estimation with Focusing on Objects and Still Seeing Surroundings

Masakazu Yoshimura  
The University of Tokyo

yoshimura4812@g.ecc.u-tokyo.ac.jp

Satoshi Ogata  
BTC Corporation, Japan

satoshi.ogata@bigtreetc.com

## Abstract

Age estimation from images can be used in many practical scenes. Most of the previous works targeted on the estimation from images in which only one face exists. Also, most of the open datasets for age estimation contain images like that. However, in some situations, age estimation in the wild and for multi-person is needed. Usually, such situations were solved by two separate models; one is a face detector which crops facial regions and the other is an age estimation model which estimates from cropped images. In this work, we propose a method that can detect and estimate the age of multi-person with a single model which estimates age with focusing on faces and still seeing surroundings. Also, we propose a training method which enables the model to estimate multi-person well despite trained with images in which only one face is photographed. In the experiments, we evaluated our proposed method compared with the traditional approach using two separate models. As the result, the accuracy could be enhanced with our proposed method. We also adapted our proposed model to commonly used single person photographed age estimation datasets and it is proved that our method is also effective to those images and outperforms the state of the art accuracy.

## 1. Introduction

Age estimation from images is an important research task because it can be used in many practical scenes like surveillance, human-robot interaction, recommendation, customer age group survey in a shop, and so on. It was also used in some other research tasks as a part of the methods. For instance, it was used to train Generative Adversarial Networks (GAN) [13] for facial age editing [39] and used to support facial recognition network [46]. It is still a challenging task mostly due to the difference be-

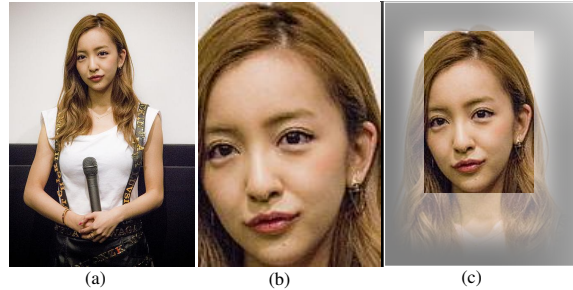


Figure 1. The visualization of the concept. (a) has the richest information, meanwhile (b) is easy to extract facial information. (c) is focusing on the face but still seeing surroundings.

tween apparent age and real age caused by genetic difference, makeup, angle, and facial expression.

In recent years, convolutional neural networks (CNN) based methods achieved great success in age estimation [42, 24, 4, 31, 17, 2]. Although their methods are varied from each other, most of their research target is to estimate from images like pictures for identification certificates in which only one face exists. However, in some situations like human-robot interaction or automatic customer age group surveys in a shop, age estimation in the wild and for multi-person is needed. Our goal of this paper is to estimate the age of multi-person in the wild accurately. Such situations were usually solved by using an additional face detector which crops facial regions and creates images to feed to the age estimator [9]. Although it might be a bit different from multi-person age estimation, [34] cropped a facial region from the huge number of wild images crawled from the internet and used them to pre-train the age estimator model. Also further tight cropping from already cropped facial datasets is commonly used as a preprocessing to align the images [42, 31, 24, 6]. Here is our idea come from. Is it optimal in terms of accuracy and efficiency to use two separate models of a detector and an age estimator and to estimate age from tightly cropped images? Though it is reasonable that alignment with tight cropping makes easy to estimate and increases the accuracy since it puts facial parts

<sup>0</sup>This work was completed while the first author was an intern at BTC Corporation.

© 2020 M. Yoshimura and S. Ogata.

always at the almost same place and puts more focus on the face, it loses some information of surrounding pixels. The information of the surrounding pixels might be useful to figure out whether the texture on the face is derived from aging, characteristic of the camera, or the environment. From these perspectives, we propose a novel model that focuses on the face the same with previous methods but, at the same time, still considers surroundings differently from previous works.

To train a multi-person age estimation model, datasets which include multi-face photographed images and corresponding annotation of the facial locations and ages are desired, but those open datasets are rare. To the best of our knowledge only Images of Groups (IoG) dataset [12] is such a dataset. However, the age annotation was defined with 7 age groups and it is too rough to make the model estimate coarsely. On the other hand, many single face photographed datasets were proposed with the rich amount and per year level annotation [44, 34, 45]. These rich and coarse datasets could be created thanks to automatic crawling from the Internet. Even if sets of multiple faces and their age information exist on the Internet, to correspond each age information to each face is difficult. So multi-person photographed dataset is difficult to create. Based on the above, we also propose a training strategy for the multi-person age estimation model. In this method, a dataset for face detection and single face photographed age estimation datasets are used to train the model.

In short, our goal is to estimate the age of multi-person accurately and the contributions of our paper are as follows:

- A novel model that can estimate the age of multi-person different from previous methods. Experiments showed that it is more accurate than using two separate models of face detection and age estimation despite having a little fewer parameters.
- The conceptual architecture of focusing on the face still somewhat considering surroundings is effective even to the images only one face is photographed and it outperformed the state-of-the-art on the two open datasets; IMDB-WIKI [34] and UTKFace [45].
- A training strategy for a multi-person age estimation model with limited datasets is proposed. It enables to train well with widely available datasets; a face detection dataset and single face photographed datasets.

## 2. Related Works

### 2.1. Face Detection

Although most of the previous age estimation methods aimed to estimate from single face photographed images, they usually utilized face detection methods to crop tightly

and align the images as a preprocessing. For example, BridgeNet [24] utilized a face detection method which could run 99 fps with a GPU [14]. Mean variance loss [31] utilized a detection method [36] which connected multiple cascade classifiers as a funnel-like structure and can process with 20 fps without using GPUs. Thus, age estimation methods for single face photographed images tend to utilize small and fast face detection method. This may be because the usual datasets for age estimation photograph only one face (although some images contain multiple faces mistakenly) and detection from them is easy.

On the other hand, deep CNN based face detection methods were proposed and beat previous methods in several years. AInnoFace [43] and RetinaFace [8] were based on RetinaNet [25] and obtained high accuracy on WiderFace dataset [37], a challenging dataset containing for face detection. In the more recent years anchor free detection methods were proposed in the field of common objects detection [47, 23]. CenterNet [47] is a keypoint based detection method and surpass RetinaNet in terms of both accuracy and speed on COCO dataset [26], a dataset for common objects detection. So, our detection part is based on CenterNet. Although [8] reported that estimating the bounding boxes with its facial landmarks enhanced the accuracy, we don't utilize facial landmarks because the gain was small and many of the age estimation datasets don't contain annotations of facial landmarks.

### 2.2. Age Estimation

As far as we know, most of the previous works were targeted on estimating age from single person photographed images. These methods can be categorized into four groups by the way of obtaining estimation. One is a method that estimates age as a regression problem [16, 15]. In other words, it tries to output the true value of the age. However, it was reported that regression methods tend to overfit the training data because apparent age and real age have a gap, and the model fit to the gaps in the training data [5]. The second one is a method which estimates age as a classification problem [33, 1, 34]. In the experiment of DEX [34], it is reported that if the amount of the training data is enough, classifying per year (classifying into 101 labels) is more accurate than regression. Also, it reported that to make the final output as the weighted average of the probability of the all age classes instead of outputting the most probable age class enhanced the accuracy. The third one outputs the probability of the ages almost the same as the classification method but treats the ordinal relationship between the age classes. C3AE [42] proposed a two-points representation way of outputs. Its age classes were rough and around per 10 ages but it could estimate coarsely from the probabilities of two adjacent classes. Also, Mean variance loss was proposed to cope with not only the ordinal information but

also the ambiguity of apparent ages by estimating possible age distributions instead of exact ages [31]. The last one is the ranking based method which classifies the ages several times from roughly to coarsely like the concept of Decision Forest [6, 24]. BridgeNet connected neighbor nodes of the tree structure and obtained robustness different from the previous ranking based methods.

Judging by the accuracy and computational burden, we created the age estimation part based on Mean variance loss [31].

### 2.3. Detection and Other Tasks in a Single Model

In other fields, several methods dealt with the detection task and subsequent other tasks in a single model. For example, several instance segmentation approaches firstly estimated bounding boxes from the feature obtained from its backbone network and then estimate segmentation masks per bounding boxes using the same feature obtained from its backbone network [18, 11]. Mask-RCNN [18] demonstrated that it was also possible to estimate human pose with the same pipeline of the instance segmentation approach. Also, an anchor free and keypoint-based detection method of CenterNet could estimate bounding boxes and human poses at one time [47]. In another field, several methods estimated the 3D pose of rigid objects together with their bounding boxes at one time [21, 40]. In the similar field to age estimation, smile recognition and facial attribute prediction were conducted at the same time with face detection [20].

Our proposed architecture is different from these previous methods in terms of using two different backbones for the detection part and the subsequent age estimation part. As described in the next section, this is more computationally efficient for age estimation.

## 3. Proposed Method

We propose a multi-person age estimation method that can detect faces and estimate their ages with a single model different from previous methods. In this section, we firstly present our model architecture that aims not only to enable multi-person age estimation but also to estimate more accurately by focusing on faces at the same time somewhat seeing the surrounding environment. Then the loss function to train the model is described. Finally, a training strategy is proposed to train the multi-person age estimation model with limiting available datasets: a face detection dataset and single face photographed datasets. This strategy is needed because creating a multi-person photographed age estimation dataset is difficult.

### 3.1. Model Architecture

An overview of our model for multi-person age estimation is shown in Fig. 2. It consists of a face detection

sub-network and an age estimation sub-network. Our motivations for this architecture are as follows. If utilizing previous single person age estimation methods on multi-person age estimation, we have to utilize other face detection method to crop faces to feed to the age estimation methods. It might be time-consuming to use two separate models. Also, the accuracy might decrease when implemented in real applications if the age estimator is overfitted to the alignment of the training data. Most of the age estimation datasets contain largely photographed faces but, in the multi-person scenario, faces are shown with small sizes. Many detectors tend to react differently against different sizes of objects due to the difference of the resolution, default anchor shapes, or how many convolution layers the features are passed through. The other motivation of the architecture is to support age estimation by the surrounding pixels. There are two connections between the detection sub-network and the age estimation sub-network. One is a facial cropping connection which is aimed to align and focus on the face to make the network easily compare different faces. The other connection is the intermediate feature connection which gives surrounding information to some extent to support age estimation. the details are as follows.

#### Facial Cropping Connection

The facial cropping connection crops facial regions corresponding to the bounding boxes estimated with the detection sub-network. This aims to align and focus on the faces similarly to previous works. We crop with some margin from bounding box estimation to be robust to the detection error. And the input images for age estimation are cropped from high-resolution images to include detail information like wrinkles. For the sake of speed and multi-process with GPU, always  $K$  most probable regions are cropped.

#### Intermediate Feature Connection

In the intermediate feature connection, the intermediate feature of the detection sub-network is transformed and mixed with the intermediate feature of the age estimation sub-network by concatenation. The transformation corresponds to cropped regions of the facial cropping connection. In other words, the corresponding regions of the intermediate feature per face are affine transformed with bilinear interpolation. Although the corresponding facial regions of the intermediate feature are extracted, these transformed features contain the information outside the regions to some extent. If  $N$  layers with  $3 \times 3$  convolutions are stacked, the possible receptive field of the one point of the last feature becomes  $(2N + 1) \times (2N + 1)$  with the center pixels in the input image more influential and the edge pixels less influential. So, by concatenating the intermediate feature, to

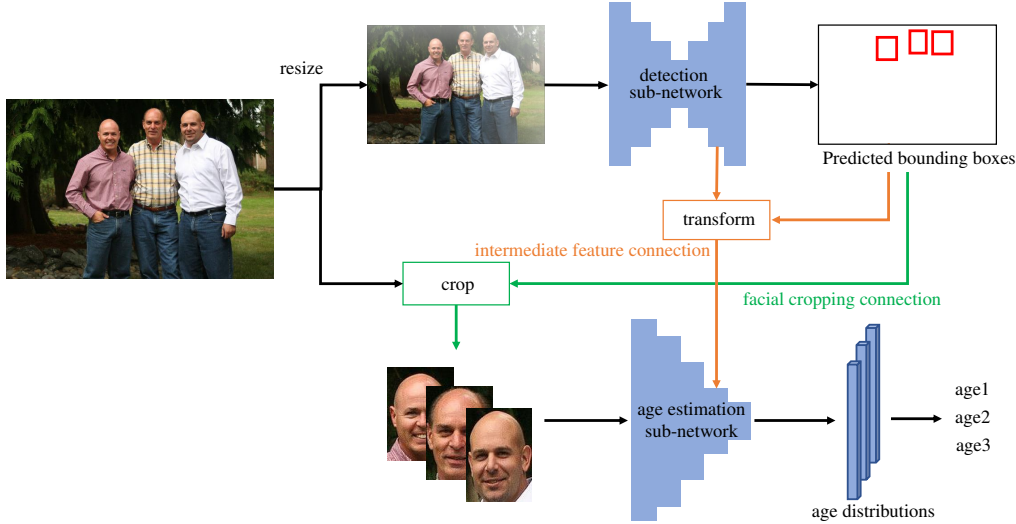


Figure 2. Overview of the proposed multi-person age estimation

estimate age with the surrounding pixel information is realized. As mentioned above, the surrounding pixels might help to judge the texture on faces is whether derived from aging, camera noise, or environments.

### Separate Backbones

Most of the previous works which dealt with detection and subsequent tasks in a single model usually shared the backbone as described in the section 2.3. Usually, it is memory efficient but, for age estimation, it is not the case because facial detailed texture like wrinkles needs to retain in the input image. For example, if we want to detect faces whose sizes are around 1/10 of the image size and  $150 \times 150$  size is needed to retain detailed texture, the input image to the shared backbone should be  $1500 \times 1500$  size. It needs heavy computation. In this context, detection and age estimation backbones are separated. To the detection backbone, resized images are input and, for the age estimation backbone, cropped images from high-resolution ones are input.

### 3.2. Loss Function

To train the model, we define multi-task loss,

$$L = L_{det} + L_{age} + L_{gen}$$

where  $L_{det}$  is a loss for the detection part and  $L_{age}$ ,  $L_{gen}$  are losses for the age and gender estimation part. Gender was also estimated with some datasets together with age in the experiments. Because we utilized CenterNet [47] as a detection sub-network in the experiments, the  $L_{det}$  is defined as,

$$L_{det} = L_{reg} + \lambda_{size}L_{size} + \lambda_{off}L_{off}$$

the same with the original method.  $L_{reg}$  is a regression loss for keypoint maps,  $L_{size}$  is a loss for bounding boxes' size, and  $L_{off}$  is a loss for sub-pixel adjustment of bounding boxes.  $\lambda_{suffix}$  denotes a weighting factor for *suffix* and it is a hyperparameter. The loss for age estimation is defined as,

$$L_{age} = \frac{1}{N_a} \sum_b^B \sum_k^K b_{iou}(\hat{d}_{b,k}, d_b) b_{age}(d_{b,k'}) \\ \times L_{age\_single}(a_{b,k}, a_{b,k'})$$

where  $B$  denotes batch size,  $K$  is the maximum number of faces per image,  $\{\hat{d}_{b,k}, d_b\}$ ,  $\{a_{b,k}, a_{b,k'}\}$  are prediction and ground truth of bounding boxes and age probability vectors.  $b_{iou}(\hat{d}_{b,k}, d_b)$  is a boolean function,

$$b_{iou}(\hat{d}_{b,k}, d_b) = \begin{cases} 1 & \max IOU > th_{iou} \\ 0 & else \end{cases}$$

in which, firstly the predicted bounding box is matched with all of the ground truth bounding boxes and calculated their intersection over union (IOU). Then, if the maximum IOU is less than a threshold  $th_{iou}$ , we mask out its value and exclude from the calculation of backpropagation. Also, the suffix  $k'$  means the ground truth whose bounding box is the best matched with  $\hat{d}_{b,k}$ . The  $b_{age}(d_{b,k'})$  is also a boolean function that masks out the value when ground truth has only bounding box annotation and no age annotation.  $L_{age\_single}(\hat{a}, a)$  is a multi-task loss composed of mean variance loss [31] and cross entropy loss,



$$L_{age\_single}(\hat{a}, a) = \lambda_{mean} L_{mean}(\hat{a}, a) + \lambda_{var} L_{var}(\hat{a}, a) + \lambda_{ce} L_{ce}(\hat{a}, a)$$

The first two terms denote mean variance loss’s components; mean loss and variance loss. The last term denotes a cross entropy loss. The  $\hat{a}$  is a per year class vector which is the output of a softmax activation. Finally, the summed up value is divided by  $N_a$ , which denotes the number of faces NOT masked out. For gender estimation, almost the same loss is used but binary cross entropy is used instead of mean variance loss and cross entropy.

$$L_{gen} = \frac{\lambda_{gen}}{N_g} \sum_b^B \sum_k^K b_{iou}(d_{b,k}, d_b) b_{gen}(d_{b,k'}) \times L_{bce}(g_{b,k}, g_{b,k'})$$

### 3.3. Training Strategy

#### End-to-End Learning or Not

Our proposed model is possible to train end-to-end with the loss function above. The merit of end-to-end learning is that the intermediate feature of the detection part can be optimized for age estimation. Meanwhile, it might cause overfitting to the training data. So, in the experiment, freezing detection sub-network while training age estimation sub-network is compared with end-to-end learning.

#### Tiling Augmentation

It is desirable to train the model with multi-person photographed datasets that have corresponding age ground truth but there are no suitable datasets like that. Moreover, it is difficult to create as mentioned above. Meanwhile, there are a lot of only face region annotated datasets and only single face photographed datasets. So we introduce tiling augmentation which utilizes the single person photographed datasets for multiple person age estimation. In this method, in order to create pseudo-multi-person photographed images, multiple images are tiled patch-wisely as shown in Fig. 3 with the number of images to use randomized. However, only feeding the tiled images might mislead the model. It might learn there is a person per patch. So we also feed the images from multiple face detection dataset which has no age labels but has seamless images. If these images are fed, the backpropagation for them in the age estimation sub-network is ignored by the boolean masking function  $b_{age}(d_{b,k'})$ .

## 4. Experiments

Our experiments roughly consist of two parts. One is the abrasion study on multi-person age estimation. The other

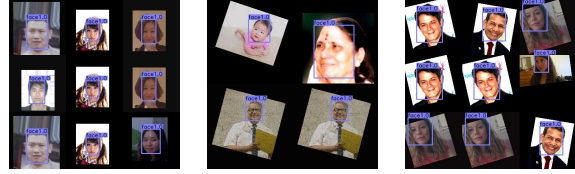


Figure 3. Two samples of tiling augmentation

is abrasion study and benchmarking on several widely used datasets that contain only one person is photographed per image.

### 4.1. Datasets

We studied our method on three datasets: Images of Groups (IoG) [12], IMDB-WIKI [34], UTKFace [45] utilizing the other three datasets: CLAP2016 [10], Mega Age Asian [44] and WiderFace [37]. We chose IoG because it is the only dataset openly available with multi-person age labels. Others were chosen because they release pre-cropped images or they have plenty of images.

**Images of Groups** consists of 5080 group images where 28,231 faces were annotated with age group labels and gender labels [12]. To the best of our knowledge, this is the only dataset releasing multi-person photographed images annotated with their ages. This dataset is challenging because face sizes are small. The median distance between the eye centers is 18.5 pixels. The definition of the age groups were 7 categories; 0-2, 3-7, 8-12, 13-19, 20-36, 37-65 and 66+. Because it is rough to estimate coarsely, we used this dataset as an evaluation dataset and didn’t train with this dataset. Also, different from previous works, we used a pre-cropped version of images.

**IMDB-WIKI** is the largest dataset with age and gender ground truth crawled from IMDB (460,723 images) and WIKI (62,328 images) [34]. The age labels are distributed from 0 to 100. Although many of the previous works [34, 6, 31] regard this dataset was not suitable for evaluation due to the noise, we compared the evaluation result with other reported results since it is one of the rare datasets which also provide pre-cropped images. Following [42], We randomly split 20 % of the data as test data and remaining as training data. By the data cleaning procedure explained bellow, we finally used 113,466 images as training data.

**UTKFace** is also one of the rare datasets that offer pre-cropped images with its age, gender, and ethnicity labels [45]. It contains over 20,000 images and the age labels are per year level from 0 to 116. we trained and evaluated with this dataset. We split 20% of the data as test data similar to previous methods [2, 4, 17], but we used from people of 0 to 100 years old as training data nonetheless they trained and evaluated with the people of 21 to 60 years old. However, we tested 21 to 60 years old people to compare with these

methods. By the data cleaning procedure, our training data was decreased from 19,285 to 18,396 images.

**CLAP2016** is the dataset which contains 7,591 images with corresponding age labels from 0 to 100 [10]. Their images have somewhat wide margin around faces. Because they also provide apparent age labels and most of the previous works compare with the apparent age estimation task, we don't evaluate on this dataset and only used for training. By the data cleaning procedure, our training data was decreased from 5,613 to 4,927 images.

**Mega Age Asian** contains 40,000 cropped facial images with age labels [44]. The age distribution is from 1 to 69. We used this dataset because the datasets above contain less Asian faces. This dataset was used only at the training phase. By the data cleaning procedure, our training data was decreased from 40,000 to 36,687 images.

**WiderFace** is a challenging dataset for face detection that contains wide variability of images in scale, pose, occlusion, expression, makeup, and illumination [37]. 32,203 images and 393,703 faces are included. We utilized this dataset to train a face detector which was used to discard some noisy training images in the age estimation dataset and create the ground truth of facial bounding boxes. Also, this dataset was used in the tiling augmentation method.

## 4.2. Implementation Details

### Data cleaning and Annotation

As described in section 2.1, we used CenterNet [47] whose backbone is DLA-34 [41] as the detection sub-network and as the annotator of facial bounding boxes. The CenterNet was trained with the training set of WiderFace dataset. Even if there are official annotations of bounding boxes in age estimation datasets, we trained the all models with the definition of WiderFace's facial bounding boxes. Many of the age estimation datasets especially the pre-cropped version of datasets sometimes contains not annotated faces in the background unconsciously and they can disturb the training of the multi-face age estimation model. So, At the annotation time of bounding boxes, we excluded images in which multiple faces are detected from the training data except those of IoG dataset. On the other hand, we didn't exclude from test data to compare the result with previous methods. Instead, we regarded the largest detected face as the target face and compared with ground truth age or gender.

### Details of Model Architecture

For the detection sub-network, images were input after resized into  $480 \times 480$ . On the other hand, for the age estimation sub-network, faces were cropped corresponding to the detections and resize into  $160 \times 224$  from high-resolution images. The cropped regions have a 20 % margin from the detected bounding boxes at the upper boundary and a 10 %

margin at the other boundaries to be robust to the detection error. In all experiments, the CenterNet is used as the detection sub-network and trained from the pre-trained weight created in the above procedure.

It was reported that VGG [35] could estimate more accurately than ResNet [19] on the age estimation task [29] and many previous works used VGG-16 as a backbone for age estimation model [31, 34, 1]. However, VGG-16 is around 4 times slower than ResNet34 and needs 4.5 times larger memory [3]. These days, TResNet is proposed which is a little faster at inference time and a little more accurate than ResNet [32]. Because multi-person age estimation in real-time needs a faster and memory-efficient model, we used TResNet instead of VGG-16. Also, we newly defined TResNet-S which had the almost same parameters with ResNet34 by decreasing the number of residual blocks from (3, 4, 11, 3) to (3, 3, 7, 3) per stage and channel width factor from 1.0 to 0.9 of TResNet-M, which has about the same parameters with ResNet50. In the case the intermediate feature connection was used, the original DCN-34's output feature before the additional skip connection added for CenterNet was branched off. The feature was 1/4 of the input size and the channel width was 48. Then, it was affine transformed into  $10 \times 14$  size per the region of bounding box prediction. Then the feature was concatenated with the output of the residual block in age estimation model whose output firstly became  $10 \times 14$ . To prove the performance improvement was not stem from increased parameters, we reduced the channel width of this residual block by 48. This results in a little light weight model. The output of the age estimation backbone was branched into two passes for age distribution prediction and gender prediction. Each pass consisted of a  $1 \times 1$  convolution layer, a global average pooling layer, a dropout layer whose dropping rate was 0.2, and a 101-way or a 2-way fully-connected layer with a softmax activation.

### Train and Test Settings

For IMDB-WIKI dataset, we trained the detection sub-network from pre-trained weight and the age estimation sub-network from scratch with adam optimizer and a batch-size of 24 for 50 epochs, while the learning rate started from  $1e-4$  and multiplied 0.1 at 30 and 40 epochs respectively. For other datasets, we trained the model from the weight trained with IMDB-WIKI with a batch-size of 12 for 80 epochs, while the learning rate started from  $1e-4$  and multiplied 0.1 at 50 and 70 epochs respectively. We applied random flip, random scaling, random crop, random rotation, color jittering, random blur as default augmentation. When tiling augmentation was applied, the number of tiles per image was randomly chosen from 1, 4, or 9. For the sake of time efficiency, maximum of four im-

ages were loaded and some tiles contained the same images. In all experiments below, hyperparameters for loss function  $\{\lambda_{size}, \lambda_{off}, \lambda_{mean}, \lambda_{var}, \lambda_{ce}, \lambda_{gen}\}$  were set as  $\{0.1, 1.0, 0.01, 0.0025, 0.05, 0.1\}$  and  $th_{iou}$  was set as 0.3. At the test time, predictions whose confidences were greater than 0.2 were regarded as faces. In the training time, the parameter  $K$ , the maximum processable number of faces, was set as 9 when tiling augmentation was applied, in other cases, set as 1 to train fast. When multiple datasets were used, we defined one epoch corresponding to the number of images in the biggest dataset, and images were chosen randomly from each dataset with the weighted probabilities based on the size of each dataset. The running time was tested on Ubuntu 18.04, Intel Xeon pratinum 8259CL processor, a Tesla T4 GPU, CUDA 10.0, python 3.6, and pytorch 1.4.

### 4.3. Ablation Study on Multi-Person Age Estimation

We tested on the test split of IoG dataset defined in [12], which contained around 20% of faces. Because the test split is based on the already cropped face images, there are mixtures of people to evaluate or not to evaluate on the same pre-cropped images. So, we estimated all faces but evaluated with only the faces for test set. The test set was balanced among age groups and gender. In these experiments, we trained the model with the training set of UTK-Face, CLAP2016, Mega Age Asian, and supporting detection dataset of WiderFace from the pre-trained weight on IMDB-WIKI. At the test time, the parameter  $K$ , the maximum processable number of faces, is set as 20 different from the training time.

The experimental results were shown in Table 1. The “baseline” was almost the same model with Mean Variance Loss [31] except using a light weight backbone. The “intermediate feature” denotes our proposed model using the intermediate feature connection aimed to consider surrounding pixels to some extent. It improved age estimation accuracy slightly despite a bit smaller model parameters but gender estimation did not improved. The tile augmentation further improved accuracy. Finally “end-to-end” denotes it was trained end-to-end meanwhile all of the above settings trained with the detection sub-network frozen. The result shows that end-to-end learning can be possible but a bit deteriorates the performance. It might be because the detection pert was also tried to estimate age and it caused overfitting. In our environment, the inference speed of the “baseline” model was 14.3 fps and that of our proposed model was 14.6 fps if the maximum detectable number  $K$  was 20. When  $K$  was set as 1, 3, 10, and 20, the inference speed were 24.3, 23.1, 18.4, and 14.6 fps respectively. Because people don’t move so fast, these speeds are enough for the usual real-time analysis.

Table 1. Ablation study on IoG dataset.

	intermediate feature	tile aug	end-to-end	accuracy [%]		
				age	1-off*	gender
baseline				38.78	79.04	<b>88.59</b>
	✓			38.87	79.30	86.83
ours	✓	✓		<b>39.71</b>	<b>81.07</b>	87.50
	✓	✓	✓	38.45	80.10	87.35

\*1-off accuracy of age group estimation

Table 2. Detail result on IoG dataset. The result using intermediate feature connection and tile augmentation is shown.

real age	0-2	3-7	8-12	13-19	20-36	37-65	66+
age	0.0	0.0	55.3	28.0	72.3	66.9	54.4
1-off	0.0	86.6	88.7	97.0	99.3	99.3	98.7
gender	79.6	84.4	82.0	87.3	97.3	98.0	98.7

From this experiment, It can be said that detecting and estimating with a single model enhance the accuracy for multi-person age estimation together with tiling augmentation.

By the way, all of the age accuracy even from the baseline model which was almost the same as the state of the art method [31] was low. We investigated the reason and it turned out that very young value and very old value can’t be output as shown in Table 2 and Fig. 4. The reason might be derived from biased distribution of training data and the mean averaging way of age output that tend to be affected by far away age classes.

### 4.4. Ablation Study on Single Person Age Estimation

Although our method is aimed to estimate multi-person, the conceptual architecture of “focusing on objects and still seeing surroundings” may be effective even if only a single face is shown in an image. So we also tested with single person photographed datasets. Firstly we conducted an ablation study again on IMDB-WIKI dataset. The results were Table 3.

Table 3. Ablation study on IMDB-WIKI dataset.

	intermediate feature	end-to-end	age	gender
			MAE	accuracy
baseline			5.87	92.23
	✓		5.82	92.18
ours	✓	✓	<b>5.64</b>	<b>92.82</b>

\*1-off accuracy of age group estimation

Even for a single person situation, our proposed method enhanced the accuracy in spite of a bit small model size. In this time, end-to-end learning enhanced the accuracy. It might be because IMDB-WIKI has a wide variety of images and hence overfitting did not occur. Our results on IMDB-WIKI were compared with the sate of the art methods in Table 5 and outperformed their accuracy. Although our model is design to be faster than usual methods, C3AE



Figure 4. Visualization of the result on IoG dataset.

[42] used much smaller model.

We also conducted an experiment on UTKFace dataset. The best method from the ablation study which used the intermediate feature connection with end-to-end learning was

Table 4. Comparison with the state of the art methods on IMDB-WIKI.

	backbone	param.*	MAE
C3AE [42]	SSR [38]	0.04M	6.91
C3AE [42]	C3AE	0.04M	6.48
[27]	multi-model	-	5.93
[28]	Xception [7]	22.9M	6.93
[28]	multi-model	-	5.89
ours	TResNet-S	19.2M	<b>5.64</b>

\* The numbers of the parameters in the age estimation backbones are listed.

Table 5. Comparison with the state of the art methods on UTKFace with 21 to 60 years old people. Our method was trained with 0 to 100 years old people different from others.

	backbone	param.	MAE
OR-CNN [30]†	ResNet34	21.8	5.74
CORAL [4]	ResNet34	21.8	5.39
DCDT [?]	ResNet50	25.6	4.65
RandomizedBins [2]	ResNet50	25.6	4.55
ours	TResNet-S	19.2	4.61
ours*	TResNet-S	19.2	<b>4.49</b>

† The result was reported in [4].

\* The model trained for IoG dataset in section 4.3 was used.

used. Our experiment was challenging because previous methods trained and tested with from 21 to 60 years old people but we trained from 0 to 100 years old people. Furthermore, only our method used pre-cropped images. This means some faces were wrongly cropped although previous methods used correctly cropped images with the help of human checks. The result is Table 4. You can see our method achieved a competitive result. Moreover, the model trained with CLAP2016 and Mega Age Asian for IoG dataset outperformed state of the art. It is interesting because in this experiment, more than half of the faces are Asian faces but UTKFace contains mostly Western faces. It can be said that even different race of faces is helpful to estimate.

## 5. Conclusion

Different from most of the previous methods, we aimed to enhance the accuracy of age estimation on multi-person photographed images. We proposed a multi-person age estimation method to cope with facial detection and age estimation in a single model. Thanks to the concept of focusing on faces and still seeing surroundings realized by facial cropping connection and intermediate feature connection, our method further improved from the baseline model which utilized state of the art method [31]. Moreover, our concept of focusing on faces and still seeing surroundings was also useful to single person photographed images and outperformed state of the art methods on IMDB-WIKI dataset and UTKFace dataset. In the future, we will examine the



effect of our method on other tasks like human pose estimation with top-down approaches which also need to detect and estimate from cropped regions.

## References

- [1] Eirikur Agustsson, Radu Timofte, and Luc Van Gool. Anchored regression networks applied to age estimation and super resolution. In *Proceedings of the IEEE International Conference on Computer Vision*, pages 1643–1652, 2017. 2.2, 4.2
- [2] Axel Berg, Magnus Oskarsson, and Mark O’Connor. Deep ordinal regression with label diversity. *arXiv preprint arXiv:2006.15864*, 2020. 1, 4.1, 5
- [3] Alfredo Canziani, Adam Paszke, and Eugenio Culurciello. An analysis of deep neural network models for practical applications. *arXiv preprint arXiv:1605.07678*, 2016. 4.2
- [4] Wenzhi Cao, Vahid Mirjalili, and Sebastian Raschka. Rank-consistent ordinal regression for neural networks. *arXiv preprint arXiv:1901.07884*, 2019. 1, 4.1, 5
- [5] Kuang-Yu Chang, Chu-Song Chen, and Yi-Ping Hung. Ordinal hyperplanes ranker with cost sensitivities for age estimation. In *CVPR 2011*, pages 585–592. IEEE, 2011. 2.2
- [6] Shixing Chen, Caojin Zhang, Ming Dong, Jialiang Le, and Mike Rao. Using ranking-cnn for age estimation. In *Proceedings of the IEEE Conference on Computer Vision and Pattern Recognition*, pages 5183–5192, 2017. 1, 2.2, 4.1
- [7] François Chollet. Xception: Deep learning with depthwise separable convolutions. In *Proceedings of the IEEE conference on computer vision and pattern recognition*, pages 1251–1258, 2017. 4
- [8] Jiankang Deng, Jia Guo, Yuxiang Zhou, Jinke Yu, Irene Kotsia, and Stefanos Zafeiriou. Retinaface: Single-stage dense face localisation in the wild. *arXiv preprint arXiv:1905.00641*, 2019. 2.1
- [9] Eran Eidinger, Roei Enbar, and Tal Hassner. Age and gender estimation of unfiltered faces. *IEEE Transactions on Information Forensics and Security*, 9(12):2170–2179, 2014. 1
- [10] Sergio Escalera, Mercedes Torres Torres, Brais Martinez, Xavier Baró, Hugo Jair Escalante, Isabelle Guyon, Georgios Tzimiropoulos, Ciprian Corneou, Marc Oliu, Mohammad Ali Bagheri, et al. Chalearn looking at people and faces of the world: Face analysis workshop and challenge 2016. In *Proceedings of the IEEE Conference on Computer Vision and Pattern Recognition Workshops*, pages 1–8, 2016. 4.1
- [11] Hao-Shu Fang, Jianhua Sun, Runzhong Wang, Minghao Gou, Yong-Lu Li, and Cewu Lu. Instaboost: Boosting instance segmentation via probability map guided copy-pasting. In *Proceedings of the IEEE International Conference on Computer Vision*, pages 682–691, 2019. 2.3
- [12] Andrew C Gallagher and Tsuhan Chen. Understanding images of groups of people. In *2009 IEEE Conference on Computer Vision and Pattern Recognition*, pages 256–263. IEEE, 2009. 1, 4.1, 4.3
- [13] Ian Goodfellow, Jean Pouget-Abadie, Mehdi Mirza, Bing Xu, David Warde-Farley, Sherjil Ozair, Aaron Courville, and Yoshua Bengio. Generative adversarial nets. In *Advances in neural information processing systems*, pages 2672–2680, 2014. 1
- [14] Guodong Guo and Guowang Mu. Joint estimation of age, gender and ethnicity: Cca vs. pls. In *2013 10th IEEE International Conference and Workshops on Automatic Face and Gesture Recognition (FG)*, pages 1–6. IEEE, 2013. 2.1
- [15] Guodong Guo, Guowang Mu, Yun Fu, and Thomas S Huang. Human age estimation using bio-inspired features. In *2009 IEEE conference on computer vision and pattern recognition*, pages 112–119. IEEE, 2009. 2.2
- [16] Guodong Guo and Xiaolong Wang. A study on human age estimation under facial expression changes. In *2012 IEEE Conference on Computer Vision and Pattern Recognition*, pages 2547–2553. IEEE, 2012. 2.2
- [17] Fredrik K Gustafsson, Martin Danelljan, Goutam Bhat, and Thomas B Schön. Dctd: deep conditional target densities for accurate regression. *arXiv preprint arXiv:1909.12297*, 2019. 1, 4.1
- [18] Kaiming He, Georgia Gkioxari, Piotr Dollár, and Ross Girshick. Mask r-cnn. In *Proceedings of the IEEE international conference on computer vision*, pages 2961–2969, 2017. 2.3
- [19] Kaiming He, Xiangyu Zhang, Shaoqing Ren, and Jian Sun. Deep residual learning for image recognition. In *Proceedings of the IEEE conference on computer vision and pattern recognition*, pages 770–778, 2016. 4.2
- [20] Youngkyoon Jang, Hatice Gunes, and Ioannis Patras. Registration-free face-ssd: Single shot analysis of smiles, facial attributes, and affect in the wild. *Computer Vision and Image Understanding*, 182:17–29, 2019. 2.3
- [21] Wadim Kehl, Fabian Manhardt, Federico Tombari, Slobodan Ilic, and Nassir Navab. Ssd-6d: Making rgb-based 3d detection and 6d pose estimation great again. In *Proceedings of the IEEE International Conference on Computer Vision*, pages 1521–1529, 2017. 2.3
- [22] Young Ho Kwon and da Vitoria Lobo. Age classification from facial images. In *Proceedings of IEEE Conference on Computer Vision and Pattern Recognition*, pages 762–767, Los Alamitos, CA, USA, jun 1994. IEEE Computer Society.
- [23] Hei Law and Jia Deng. Cornernet: Detecting objects as paired keypoints. In *Proceedings of the European Conference on Computer Vision (ECCV)*, pages 734–750, 2018. 2.1
- [24] Wanhua Li, Jiwen Lu, Jianjiang Feng, Chunjing Xu, Jie Zhou, and Qi Tian. Bridgenet: A continuity-aware probabilistic network for age estimation. In *Proceedings of the IEEE Conference on Computer Vision and Pattern Recognition*, pages 1145–1154, 2019. 1, 2.1, 2.2
- [25] Tsung-Yi Lin, Priya Goyal, Ross Girshick, Kaiming He, and Piotr Dollár. Focal loss for dense object detection. In *Proceedings of the IEEE international conference on computer vision*, pages 2980–2988, 2017. 2.1
- [26] Tsung-Yi Lin, Michael Maire, Serge Belongie, James Hays, Pietro Perona, Deva Ramanan, Piotr Dollár, and C Lawrence Zitnick. Microsoft coco: Common objects in context. In *European conference on computer vision*, pages 740–755. Springer, 2014. 2.1
- [27] Kuan-Hsien Liu, Pak Ki Chan, and Tsung-Jung Liu. Smart facial age estimation with stacked deep network fu-

- sion. In *2018 IEEE International Conference on Consumer Electronics-Taiwan (ICCE-TW)*, pages 1–2. IEEE, 2018. 4
- [28] Kuan-Hsien Liu, Hsin-Hua Liu, Pak Ki Chan, Tsung-Jung Liu, and Soo-Chang Pei. Age estimation via fusion of depth-wise separable convolutional neural networks. In *2018 IEEE International Workshop on Information Forensics and Security (WIFS)*, pages 1–8. IEEE, 2018. 4
- [29] Arafat Abu Mallouh, Zakariya Qawaqneh, and Buket D Barkana. Utilizing cnns and transfer learning of pre-trained models for age range classification from unconstrained face images. *Image and Vision Computing*, 88:41–51, 2019. 4.2
- [30] Zhenxing Niu, Mo Zhou, Le Wang, Xinbo Gao, and Gang Hua. Ordinal regression with multiple output cnn for age estimation. In *Proceedings of the IEEE conference on computer vision and pattern recognition*, pages 4920–4928, 2016. 5
- [31] Hongyu Pan, Hu Han, Shiguang Shan, and Xilin Chen. Mean-variance loss for deep age estimation from a face. In *Proceedings of the IEEE Conference on Computer Vision and Pattern Recognition*, pages 5285–5294, 2018. 1, 2.1, 2.2, 3.2, 4.1, 4.2, 4.3, 4.3, 5
- [32] Tal Ridnik, Hussam Lawen, Asaf Noy, and Itamar Friedman. Tresnet: High performance gpu-dedicated architecture. *arXiv preprint arXiv:2003.13630*, 2020. 4.2
- [33] Pau Rodríguez, Guillem Cucurull, Josep M Gonfaus, F Xavier Roca, and Jordi González. Age and gender recognition in the wild with deep attention. *Pattern Recognition*, 72:563–571, 2017. 2.2
- [34] Rasmus Rothe, Radu Timofte, and Luc Van Gool. Dex: Deep expectation of apparent age from a single image. In *IEEE International Conference on Computer Vision Workshops (ICCVW)*, December 2015. 1, 2.2, 4.1, 4.2
- [35] Karen Simonyan and Andrew Zisserman. Very deep convolutional networks for large-scale image recognition. *arXiv preprint arXiv:1409.1556*, 2014. 4.2
- [36] Shuzhe Wu, Meina Kan, Zhenliang He, Shiguang Shan, and Xilin Chen. Funnel-structured cascade for multi-view face detection with alignment-awareness. *Neurocomputing*, 221:138–145, 2017. 2.1
- [37] Shuo Yang, Ping Luo, Chen Change Loy, and Xiaoou Tang. Wider face: A face detection benchmark. In *IEEE Conference on Computer Vision and Pattern Recognition (CVPR)*, 2016. 2.1, 4.1
- [38] Tsun-Yi Yang, Yi-Hsuan Huang, Yen-Yu Lin, Pi-Cheng Hsiu, and Yung-Yu Chuang. Ssr-net: A compact soft stage-wise regression network for age estimation. In *IJCAI*, volume 5, page 7, 2018. 4
- [39] Xu Yao, Gilles Puy, Alasdair Newson, Yann Gousseau, and Pierre Hellier. High resolution face age editing. *arXiv preprint arXiv:2005.04410*, 2020. 1
- [40] M. Yoshimura, M. M. Marinho, K. Harada, and M. Mitsuishi. Single-shot pose estimation of surgical robot instruments’ shafts from monocular endoscopic images. In *2020 IEEE International Conference on Robotics and Automation (ICRA)*, pages 9960–9966, 2020. 2.3
- [41] Fisher Yu, Dequan Wang, Evan Shelhamer, and Trevor Darrell. Deep layer aggregation. In *Proceedings of the IEEE conference on computer vision and pattern recognition*, pages 2403–2412, 2018. 4.2
- [42] Chao Zhang, Shuaicheng Liu, Xun Xu, and Ce Zhu. C3ae: Exploring the limits of compact model for age estimation. In *Proceedings of the IEEE Conference on Computer Vision and Pattern Recognition*, pages 12587–12596, 2019. 1, 2.2, 4.1, 4.4, 4
- [43] Faen Zhang, Xinyu Fan, Guo Ai, Jianfei Song, Yongqiang Qin, and Jiahong Wu. Accurate face detection for high performance. *arXiv preprint arXiv:1905.01585*, 2019. 2.1
- [44] Yunxuan Zhang, Li Liu, Cheng Li, et al. Quantifying facial age by posterior of age comparisons. *arXiv preprint arXiv:1708.09687*, 2017. 1, 4.1
- [45] Zhifei Zhang, Yang Song, and Hairong Qi. Age progression/regression by conditional adversarial autoencoder. In *Proceedings of the IEEE conference on computer vision and pattern recognition*, pages 5810–5818, 2017. 1, 4.1
- [46] Tianyue Zheng, Weihong Deng, and Jiani Hu. Age estimation guided convolutional neural network for age-invariant face recognition. In *Proceedings of the IEEE Conference on Computer Vision and Pattern Recognition Workshops*, pages 1–9, 2017. 1
- [47] Xingyi Zhou, Dequan Wang, and Philipp Krähenbühl. Objects as points. In *arXiv preprint arXiv:1904.07850*, 2019. 2.1, 2.3, 3.2, 4.2